Organic Photovoltaics with Carbon Nanotube Charge Collectors: Inverted Structures for Parallel Tandems

Kamil Mielczarek[1], Alexander Cook[1], Anvar Zakhidov[1], Senku Tanaka[2], Ichiro Hiromitsu[2], and Katsumi Yoshino[3]

[1]*Alan G. MacDiarmid Nanotech Institute, University of Texas at Dallas, Richardson, Texas, USA*
[2]*Shimane University, Matsue, Shimane, Japan*
[3]*Shimane Institute for Industrial Technology, Matsue, Shimane, Japan*

Abstract

In order to achieve higher power conversion efficiencies within organic photovoltaics (OPVs), more solar light must be absorbed from a broader spectrum. We demonstrate that OPVs with different photoactive layers can be connected in parallel to form monolithic tandems using mechanically strong, electrically conductive, and transparent networks of carbon nanotubes as charge collectors. We show how our earlier results on such parallel tandems [1] can be significantly improved by using the inverted OPV structures with charge selective layers of inorganic oxide films. Such robust inorganic layers allow inverting the usual Indium Tin Oxide (ITO) anode into a cathode, and also protect it from electrical shorting by sharp carbon nanotubes (CNTs) nanoneedles. To further improve OPV tandems we show how doping affects CNTs to lower their sheet resistance as well as reducing the incidence of shorting within the small molecule sub-cell.

1 Introduction

Organic photovoltaics have been the focus of much research as a potential source of cheap renewable energy for many different applications. They are attractive due to the ease of processing, use of abundant materials, and the possibility of roll-to-roll manufacturing. However, the record power conversion efficiency (PCE) for OPVs is just over 8% for single junction polymeric cells [2], and over 9% for series connected small molecule cells [3], which is still below the 10% limit needed for various market applications. OPVs are hindered due to a short exciton diffusion length ($L_D \sim 10$ nm), resulting in recombination of excitons generated further than the diffusion length from an acceptor molecule. This small L_D requires either very thin active layers or mixed donor-acceptor architectures with nanoscale control of the morphology. Similarly, a short charge carrier mean free path, $L_F \sim 100$ nm, results in many photogenerated charges (electrons and holes) recombining before they reach collecting electrodes which are placed at distances larger than L_F. This small $L_F < 100$ nm limits the thickness of photoactive layers in OPVs, decreasing their efficiency and lifetime as less light is absorbed due to a reduced thickness. Unlike inorganic semiconductors the fine band structure of organic materials limits the width of the absorption spectrum and prevents broadband absorption.

Within polymeric photovoltaics (PPVs), the problem of short diffusion lengths for both excitons and charges has received much attention. Groups have focused on improving the nanoscale morphology through the use of thermal annealing [4], slow drying [5], and special additives [6] within the bulk heterojunction. All these processing steps have helped improve both device performance and an understanding of the behavior of excitons within the polymer-fullerene matrix, but they do not address the problem caused by the limited spectral coverage of many polymers.

Groups have created many copolymers with alternating donor and acceptor blocks resulting in a smaller optical band gaps [7]. However, in many cases this reduction of the band gap has only red shifted the absorption spectrum of the polymer instead of creating the desired broadband absorber capable of covering the entire spectral region. One solution is to use multiple polymers stacked within a single device such that each polymer's absorption spectra complements one another.

We propose the use of semi-transparent carbon nanotube sheets as electrodes to enhance charge collection within the bulk heterojunction and to function as an electrode within multi-junction devices. We have shown that using a porous carbon nanotube network within the photoactive layers collects more charges, as the sheets act as 3D porous electrodes which may allow for thicker devices without charges recombining due to the short L_F [8]. Secondly, the nanotube sheets make excellent transparent interlayer electrodes in series and parallel tandem solar cells due to their high transparency, low resistance, and processing compatibility.

Stacked cells can be configured in either series or par-

allel configurations. In the series configuration, the junction between two different photoactive regions acts as a recombination site for holes from one sub-cell and electrons from the other. The result is a configuration in which the open circuit voltage (V_{OC}) is the sum of the open circuit voltages for each sub cell while the short circuit current (J_{SC}) will be limited by the smaller J_{SC} of the two sub-cells. In the parallel configuration, the junction between each photoactive region will act as either a common anode or cathode. The J_{SC} will be the sum of the two sub-cells' J_{SC} while the V_{OC} will be between the lowest and the highest, depending on the filling factors of each sub-cell and any contact resistance incurred by the interlayer electrode. Series connections require careful optimization of each active layer in order to achieve a balance of the currents within the two cells. Conversely, parallel tandem cells do not require such careful considerations as the V_{OC} of the sub-cells do not depend on incident light intensity and tend to be similar for most organic materials, allowing high efficiencies to be more quickly realized.

2 Fullerene Based Molecules as Electron Acceptors in High Performance Organic Photovoltaics

The discovery 20 years ago at Osaka University (by Yoshino and Zakhidov team) that the C_{60} fullerene molecule can strongly suppress photoluminescence of various poly-alkyl-thiophenes (PAT) [9–11], poly-hexyl-thiophenes (PHT) [12], poly-octyl-thiophenes (POT) [13] and other conjugated polymers such as poly(p-phyenylenevinylene) derivatives and polyacetylene derivatives [13–15], has been critical towards an understanding of the photophysics within conjugated polymer-fullerene systems. Upon this discovery, it was immediately suggested that either photoinduced charge transfer (PCT) from the PAT polymer to C_{60}, or energy transfer from an exciton on the PAT polymer chain to C_{60} molecule, can be responsible for such a phenomenon [9–13, 15]. In order to uncover which mechanism is responsible for this effect, the photoconductivity of PAT/C_{60} mixtures was studied and a strong enhancement of the photoconductivity was discovered [14–17], which proved that the primary means of the charge transfer mechanism is indeed an exciton dissociation process on C_{60}, followed by electron transfer to the π-electron system of the fullerene. The Osaka group showed that an increased concentration of holes on PAT chains is responsible for the increased photoconductivity [18]. Photocells using planar layers of PAT on thin films of C_{60} were used to study the spectral dependence of PAT/C_{60} systems [14, 19, 20]. The effect was extended to C_{70} and higher fullerenes [18, 20–22], and it was shown that such higher fullerenes exhibit weaker PCT, as compared to C_{60}.

Detailed studies into the mechanisms of photoinduced charge transport were made by Yoshino and Zakhidov [23–27]. Belt polaron formation on the ideally symmetric sphere of C_{60} was suggested to be responsible for ultrafast PCT [19, 20], and accompanied suppression of back transfer from the C_{60}^{-} ion to PAT^{+}, due to polaronic self-trapping and spatial localization of the polaron. The formation of a belt polaron has been suggested as a further step in PCT [28]. Later experiments on both bulk heterojunction and planar organic photocells with C_{60} proved the existence and importance of resonant energy transfer from the conjugated polymer chains to C_{60}, followed by back hole transfer from C_{60}^{*} to the polymer chain. This process was called "energy-charge transfer ping-pong," and is now being carefully studied in OPVs as a mechanism of superior charge transfer from donor polymers and small molecules, to acceptor C_{60} fullerene molecules and fullerene derivatives [29]. More detailed studies will further clarify the role of C_{60} in PCT with different classes of conjugated polymers within OPVs, and other related systems (photodetectors, etc). There is no doubt that the physics of C_{60}'s π-electronic cloud is unusually rich, due to its high symmetry and self-trapping effects. Such electronic features of C_{60} are responsible for a number of exciting effects; filling of the π-electron band with 3 electrons (e.g. donated from alkali metal dopant) leads to superconductivity in alkali-doped fullerides [30–32], while only single electron filled bands induces ferromagnetic ordering in tetrakis(dimethylamino)ethylene-C_{60} (TDAE-C_{60}) [33]. It is not surprising that electron mobility within C_{60} molecular networks in the bulk heterojunctions of OPVs is higher than the hole mobility for many polymers, including highly crystalline P3HT. Based on these fundamental studies the Yoshino and Zakhidov group proposed many novel concepts and device structures to realize highly efficient photovoltaic devices with conducting polymers/fullerene structures [34–37].

3 Previous Work on Parallel OPV Tandems

In our previous work [1], we reported a monolithic parallel tandem which utilized a transparent multiwalled carbon nanotube (MWNT) interlayer electrode and complementing absorbing layers comprised of a Poly (3-Hexylthiophene) (P3HT):[6,6]-phenyl-C_{61}-butyric acid methyl ester bulk hererojunction (PCBM) polymeric front cell (green absorber) and a Copper Phthalocyanine (CuPc):C_{60} small molecule back cell (red absorber). The device is shown schematically in Figure 1. The bottom cell is electrically "inverted" when compared to conventional cells: ITO functions as a cathode while the carbon nanotube interlayer is a common anode. The difference between the work functions of ITO (~4.8 eV) and MWNT (~5.2 eV) is relatively small, thus the internal electric field which helps photogenerated charges

move towards appropriate electrodes is also small. Without the guiding influence of a strong internal electric field, photogenerated charges could move to either electrode within the P3HT:PCBM active layer. This can result in recombination as evident in reduced current as well as losses in the front cell's filling factor (FF). A thin layer of Poly(3,4-ethylenedioxythiophene) poly(styrenesulfonate) (PEDOT:PSS) was introduced on either side of the MWNT sheet to act as an electron blocking layer and to increase the contact area by filling in voids between bundles of carbon nanotubes. It was noted that the performance of the front cell improved by 24% when the top electrode was sandwiched between layers of PEDOT:PSS rather than just a single layer of PEDOT:PSS. The performance of this cell is modest and is shown in Table 2 as devices A, B and C, but it demonstrates the concept of a parallel tandem cell: the current and efficiency was larger than that of each individual cell but not exactly the sum. These losses are attributed to resistive losses at the interlayer electrode and significant shunts through the thin small molecule top cell by CNTs protruding from the electrode. From the external quantum efficiency, it is clear that the tandem cell has spectral contributions from both the P3HT:PCBM front cell, in the range of 400-650nm, and from the CuPc:C_{60} back cell, in the range of 600-750nm. Additionally, due to the contact resistance between the MWNT and organic layers, the front cell had a small internal electric field due to the similar work functions of the two electrodes. It was suggested that a different choice in transparent conducting oxide would help with the internal electric field, however, this is not required; only proper inversion of the bottom cell using charge selective layers is required.

There are three major tasks to improve the performance of this basic parallel tandem device. First, we need to improve the quality of the inverted front cell with inversion layers. Secondly, we must improve the conductivity and transparency of the interlayer electrode. Finally, we need to improve the fabrication of the back cell so that the roughness of the front cell and CNT interlayer electrode do not result in many shorts.

4 Inorganic Inversion Layers

In order to improve the performance of the previous tandem, the front polymeric cell must be properly inverted, using improved inversion and charge selective layers. The first concern is that PEDOT:PSS is dispersed in water while the polymeric layers are hydrophobic. This mismatch in surface energies produces nonuniform layers with many defects. Even when mixed with three parts methanol, PEDOT:PSS does not form high quality, continuous films on top of polymers. This can cause pinholes, shunts, and recombination sites. As a replacement to PEDOT:PSS, there are several semiconducting metal oxides available which can function as an electron blocking and hole transport layer (HTL); examples include V_2O_5, MoO_3 and WO_3. To evaluate the effectiveness of Molybdenum Trioxide as a hole transport/electron blocking layer, conventionally structured devices were fabricated on ITO (15 $\Omega/\square$) which had a MoO_3 layer coated on top instead of PEDOT:PSS. A P3HT:PCBM bulk heterojunction and an Aluminium top electrode finished the devices. Various thicknesses of MoO_3 were tested, from 0 nm to 30 nm. The devices' schematic band structure and JV curves are shown in Figure 2, and device performance under 100 mW/cm^2 AM1.5G illumination is shown in Table 2 as devices D-G. With the inclusion of a thin 10 nm thick layer of MoO_3, the device can achieve a high PCE. The FF is comparable to that of devices in which PEDOT:PSS was used, and the JV curves lack the S-type shape representative of charge build up at interfaces [38]. It is clear that MoO_3 can be used as a replacement to PEDOT:PSS. As the thickness of MoO_3 increases, there is a subtle decrease in the current of the device which is due to the overlapping absorption spectrum of both MoO_3 and the polymer.

Inverting the ITO anode into a cathode is best accomplished by metal oxides such as titanium dioxide or zinc oxide. Titanium dioxide has been demonstrated in dye sensitized solar cells with great success [39] when in the anatase crystalline phase due to its high photoconductivity and electron mobility. However, these characteristics require sintering at temperatures in excess of 350 °C [40], which is too high for organic materials. Zinc oxide nanoparticles (ZnO-NP) have been demonstrated as an alternative to fullerenes within an acceptor in bulk heterojunction devices [41] and are a strong candidate as an n-type charge selective layer for use in inverted solar cells. ZnO-NPs are simple to synthesize, can be dispersed in alcohols, and do not require any further treatment such as annealing, sintering, or hydrolysis after deposition [42]. The ZnO-NPs are a wide band gap inorganic semiconductor, and thus can provide a large optical window for incoming photons to be absorbed within the photoactive polymeric layers. Additionally, a deep HOMO level prevents holes from reaching the cathode.

To evaluate the effectiveness of the zinc oxide nanoparticles, we fabricated conventionally structured devices in which a layer of ZnO-NP was spin-coated on top of the polymer to form a hole blocking layer. The device schematic and resulting JV curves are shown in Figure 3, while device characteristics are tabulated in Table 2 as devices H-K. The JV curves show a high J_{SC}; this is only possible if the ZnO-NPs have electron mobilities comparable or larger than the fullerene network within the bulk heterojunction. Otherwise, there would be charge build up and the JV curves would show an S-shape [38].

To test the effectiveness of ZnO-NPs and MoO_3 as inversion layers for the front cell of the tandem, several inverted single junctions were fabricated. The robustness of this configuration was demonstrated by using two different transparent conducting oxides; fluorinated tin oxide (FTO) and ITO, with work functions ~4.4 eV

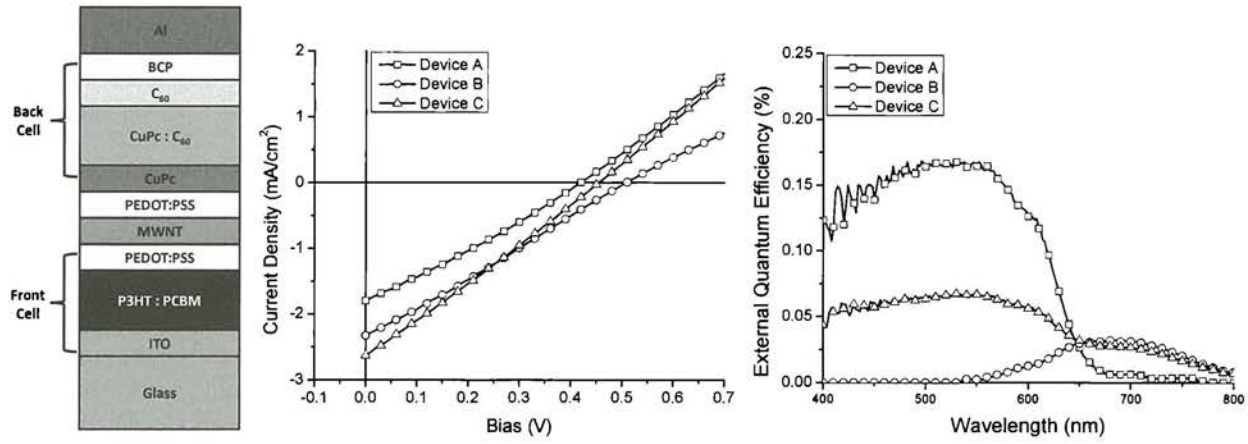

Figure 1: Device structure diagram (Left), J-V characteristic (Center) and external quantum efficiency (Right) of Tanaka et. al. parallel tandem OPV.

and ~4.8 eV, respectively, were used as cathodes. Similarly, the anodes were varied using gold and aluminum with work functions of 5.1 eV and 4.1 eV, respectively. The device schematics and JV characteristics are shown in Figure 4, with performance characteristics shown in Table 2 as devices L-N. Remarkably, all configurations show nearly identical JV characteristics despite having different anode and cathode materials. The different electrode materials would normally change the internal electric field and could, in the case of ITO/Al, have an electric field that is opposite to the preferred direction for charges to travel. However, the use of the charge selective layers essentially screens the electric field due to the electrodes, and generates a new electric field from the LUMO level of ZnO-NP (~4.4 eV) and the HOMO level of MoO_3 (~5.4 eV), as compared to the electric field which would have been seen with ITO (~4.4 eV) and Al (~4.1 eV).

After producing high quality inverted devices with conventional electrodes, inverted devices with semi-transparent nanotube electrodes were developed. For this purpose, we employed single walled carbon nanotubes (SWNT) which have higher conductivities and transparency than the MWNTs we used previously. The SWNT films are named after the number of minutes that nanotubes were collected within the reactor; the longer the duration, the more opaque and conductive the nanotube films. Table 1 shows three typical samples' sheet resistance and transmittance [43]. To form a transparent anode, SWNT sheets were laminated on top of a MoO_3 film on an inverted device similar in structure to those described previously. The devices were measured, with the illuminated electrode being noted within the parenthesis of Figure 5, and device performance characteristics are noted in Table 2 as devices O-R. The "16min" sample (having a sheet resistance of 200 Ω/□ and transmittance of 60%) shows the highest performance when illuminated through the highly transparent ITO layer due to the SWNT's low sheet resistance. However, when illuminated through the SWNT side, a 40% reduction in the current is seen and the fill factor is reduced. This is not the case for the more transparent sample, "8min," which has a sheet resistance of 500 Ω/□ and transmittance of 90%; this device shows nearly the same performance when illuminated through either the ITO or SWNT, as the electrodes are almost equally transparent. Using ZnO-NP and MoO_3 as charge selective layers resolves many of the problems from the previous front cell; these materials are robust and compatible with nanotube device architectures and will allow for higher efficiency tandem structures.

5 Doping of Carbon Nanotubes using F_4-TCNQ

To improve the conductivity of the carbon nanotubes and to produce thick hole transport layers in small molecule OPVs, we employed P-Type doping with the organic acceptor molecule tetrauoro-tetracyano-quinodimethane (F_4-TCNQ) [44–46]. It is possible to do this type of doping by a solution method in which the F_4-TCNQ is dissolved in a solvent and applied to the nanotubes, or via thermal evaporation. Our experiments have shown a four-fold increase in the conductivity of SWNTs coated with this molecule, while sheets of MWNTs show an improvement in conductivity of up to 50%. For the less transparent sheets, this doping may reduce the sheet resistance below 100 Ω/□, while not affecting the sheet's overall transparency.

Doping by sublimation in high vacuum was employed in these tandem devices, as the same dopant can be used to simultaneously dope the carbon nanotubes and hole transport layer. The total doping effect is less than that of the solution method, with only a two-fold improvement in conductivity, as there is less coverage of the nanotubes.

Using the hole transport material N,N,N,N-

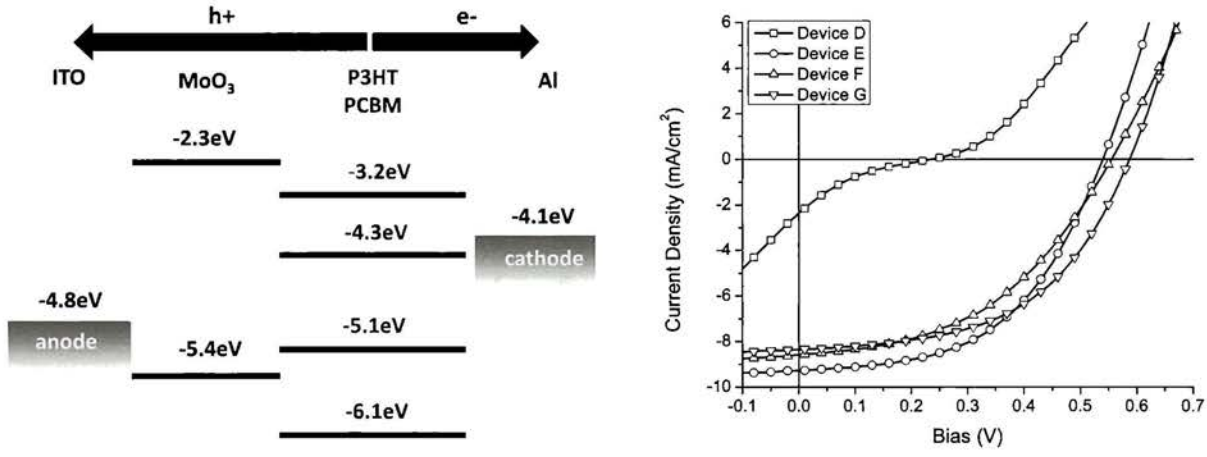

Figure 2: The energy band diagram (Left) and the J-V characteristics (Right) for a traditional cell with MoO_3 as the hole transport layer.

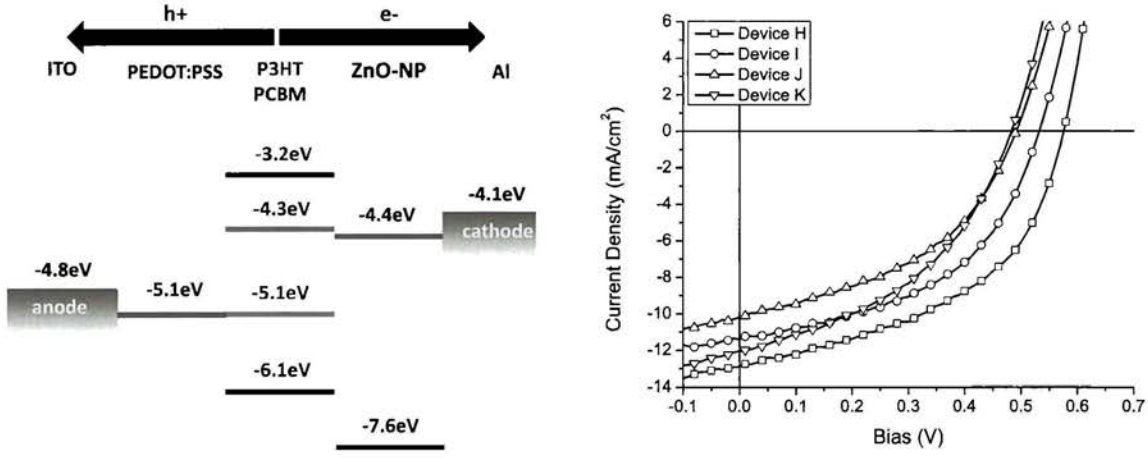

Figure 3: The energy band diagram (Left) and the J-V characteristics (Right) for a traditional cell with PEDOT:PSS as the hole transport layer and ZnO-NPs introduced as an electron transport layer.

Tetrakis(4-methoxyphenyl)-benzidine (MeO-TPD), and F_4-TCNQ as a p-type dopant, 50 nm thick hole transport layers were created by co-depositing each material, producing a hole transport layer with high conductivity and optical transparency. Devices fabricated on ITO substrates with a thick p-doped hole transport layer show no loss in performance when compared to devices without the hole transport layer. This type of doping and the ability to deposit thicker films is important when building the back cell of the parallel tandem stack because such thick HTLs provide a larger separation between the interlayer SWNTs and the top electrode, thus preventing any shunts and minimizing leakage current. Furthermore, the doped HTL also dopes the SWNT interlayer electrode, increasing the conductivity without any optical losses.

6 Tandem Cell with SWNT Interlayer Electrode

By incorporating the improvements within the polymeric sub-cell in the form of charge selective inversion layers and the doped layers of the small molecule sub-cell, we fabricated a parallel tandem cell utilizing highly transparent and conductive SWNTs as an interlayer electrode. The device layer structure is shown in Figure 6. The front cell of the tandem was built on top of patterned ITO (15 $\Omega/\square$) which had a thin layer of ZnO-NP spin-coated on top. The green absorbing photoactive layer is composed of P3HT donor and PCBM accepter molecules. A hole transport layer, MoO_3, was vacuum deposited on top of the polymeric stack, and SWNTs were laminated on top to form the front sub-cell. The device was placed into a vacuum system in which the small molecule cell was fabricated. First, a 50 nm hole transport layer of MeO-TPD doped by F_4-TCNQ (p-MeO-TPD) was evaporated, followed by 5 nm of CuPc, and a 60 nm thick layer of co-

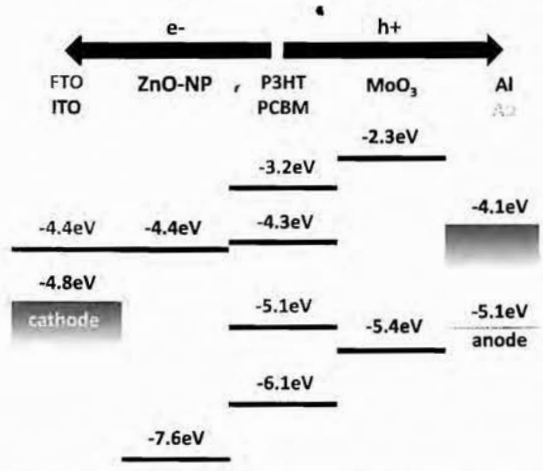

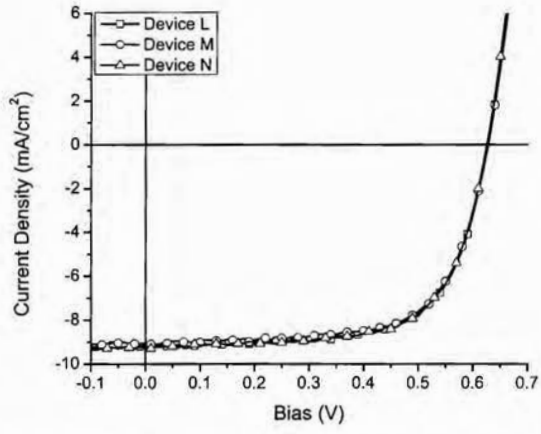

Figure 4: The energy band diagram (Left) and the J-V characteristics (Right) for an inverted cell with MoO_3 as the hole transport layer and ZnO-NPs as an electron transport layer demonstrating the freedom of electrodes for both cathode and anode.

deposited CuPc and C_{60}. An additional 5 nm of C_{60} was evaporated, followed by 10 nm of the electron transport material, bathrocuproine (BCP). The device was masked and 100 nm of Aluminium was deposited as the top cathode.

Individual sub-cells were characterized under 100 mW/cm^2 AM1.5G simulated sunlight. The JV curve is shown in Figure 6, and the device characteristics are summarized in Table 2 as devices S-U. This device demonstrates significant improvements to the previous attempt and demonstrates a short circuit current that is closer to the sum of the individual sub-cells. Furthermore, using proper inversion layers and a doped hole transport layer, the device's diode behavior is improved and the fill factors are higher. The voltage loss could be reduced by using sub-cells with better matched open circuit voltages, or through changing of the built-in potential by introducing n-type and p-type dopants within the small molecule cell.

7 Conclusion

We have presented a sequential analysis of the performance of our previous device and improved upon the design through the use of charge selective layers within the polymeric stack, doped SWNT interlayers, and a doped hole transport layer within the small molecule stack. The introduction of charge selective layers efficiently inverts the polarity of the front cell while maintaining a high and properly oriented electric field which facilitates efficient charge collection for the green light absorbing P3HT:PCBM sub-cell. The introduction of a doped hole transport layer decreases the incidence of shorting and dopes the single walled carbon nanotubes. These modifications resulted in a 600% improvement in power conversion efficiency: from 0.31% to 2.26%. These improvements were achieved while also demonstrating the enhanced spectral sensitivity and addition of short circuit currents from the two sub-cells.

Duration minutes	Transmission %	Sheet Resistance Ω/□
16	60	200
12	80	300
8	90	500

Table 1: SWNT deposition duration and the resulting electrical and optical properties

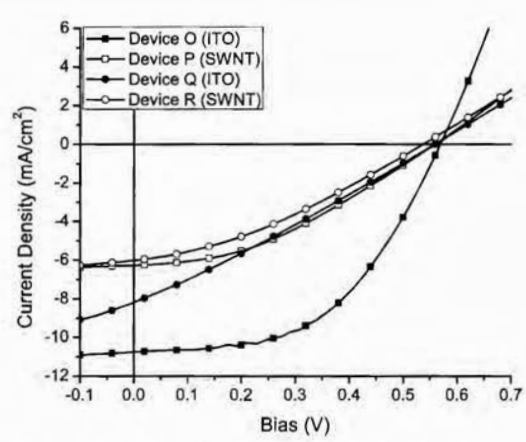

Figure 5: The JV characteristics for two devices based on illumination from either the ITO or the SWNT electrode

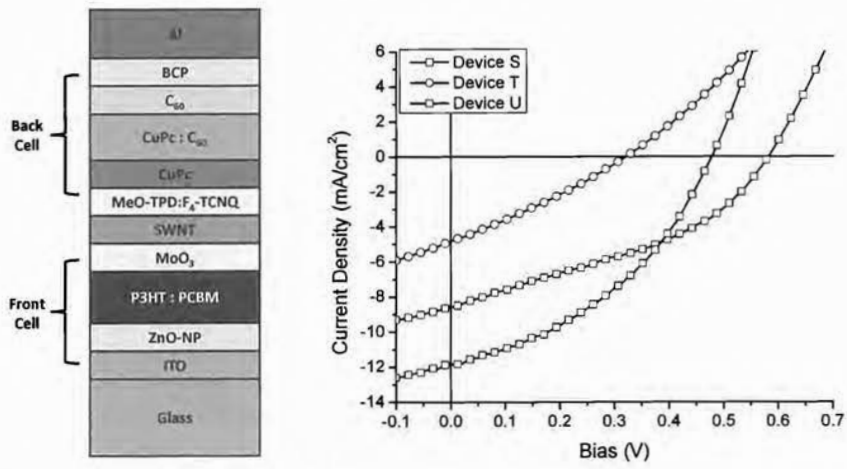

Figure 6: Device structure diagram (Left), J-V characteristic (Right) for a parallel tandem with improved bottom cell inversion and a doped hole transport layer within the back cell.

Device	HTL	ETL	Anode	Cathode	V_{OC} V	J_{SC} mA/cm^2	FF	η %	Notes
Tandem									
A	PEDOT:PSS	None	MWNT	ITO	0.51	2.3	0.26	0.30	Front Cell [1]
B		BCP		Al	0.42	1.8	0.28	0.21	Back Cell [1]
C				ITO/Al	0.46	2.6	0.26	0.31	Parallel Tandem [1]
Regular									
D	None	None	ITO	Al	0.24	2.4	0.14	0.08	
E	MoO_3, 10nm				0.54	9.3	0.51	2.56	
F	20nm				0.56	8.6	0.45	2.18	
G	30nm				0.59	8.3	0.51	2.54	
Regular									
H	PEDOT:PSS	ZnO-NP, 1500RPM	ITO	Al	0.58	12.9	0.47	3.53	
I		2000RPM			0.54	11.4	0.47	2.91	
J		2500RPM			0.50	10.2	0.43	2.11	
K		3000RPM			0.49	12.0	0.42	2.50	
Inverted									
L	MoO_3	ZnO-NP	Al	ITO	0.63	9.2	0.67	3.91	
M			Au		0.63	9.1	0.66	3.82	
N			Al	FTO	0.63	9.3	0.66	3.88	
Inverted									
O	MoO_3	ZnO-NP	SWNT, 16min	ITO	0.56	10.7	0.51	3.12	ITO Side
P					0.56	6.2	0.37	1.31	SWNT Side
Q			SWNT, 8min	ITO	0.56	8.2	0.27	1.25	ITO Side
R					0.54	6.0	0.33	1.09	SWNT Side
Tandem									
S	MoO_3	ZnO-NP	SWNT, 8min	ITO	0.59	9.0	0.38	1.89	Front Cell
T	p-MeO-TPD	BCP		Al	0.32	4.9	0.29	0.45	Back Cell
U	MoO_3/p-MeO-TPD	BCP/ZnO-NP		ITO/Al	0.48	11.8	0.40	2.26	Parallel Tandem

Table 2: A summary of device photovoltaic properties under simulated AM1.5G sunlight

References

[1] S. Tanaka, K. Mielczarek, R. Ovalle-Robles, B. Wang, D. Hsu, and A. A. Zakhidov, "Monolithic parallel tandem organic photovoltaic cell with transparent carbon nanotube interlayer," *Applied Physics Letters*, vol. 94, no. 11, p. 113506, 2009.

[2] Y. Liang, Z. Xu, J. Xia, S.-T. Tsai, Y. Wu, G. Li, C. Ray, and L. Yu, "For the Bright Future-Bulk Heterojunction Polymer Solar Cells with Power Conversion Efficiency of 7.4%," *Advanced Materials*, pp. E135–E138, Jan. 2010.

[3] H. GmbH., "Heliatek achieves new world record for organic solar cells with certified 9.8 cell efficiency." http://www.heliatek.com/, Dec. 2010.

[4] F. Padinger, R. Rittberger, and N. Sariciftci, "Effects of Postproduction Treatment on Plastic Solar Cells," *Advanced Functional Materials*, vol. 13, pp. 85–88, Jan. 2003.

[5] G. Li, V. Shrotriya, J. Huang, Y. Yao, T. Moriarty, K. Emery, and Y. Yang, "High-efficiency solution processable polymer photovoltaic cells by self-organization of polymer blends," *Nature Materials*, vol. 4, pp. 864–868, Oct. 2005.

[6] J. Peet, J. Y. Kim, N. E. Coates, W. L. Ma, D. Moses, A. J. Heeger, and G. C. Bazan, "Efficiency enhancement in low-bandgap polymer solar cells by processing with alkane dithiols.," *Nature materials*, vol. 6, pp. 497–500, July 2007.

[7] E. Bundgaard and F. Krebs, "Low band gap polymers for organic photovoltaics," *Solar Energy Materials and Solar Cells*, vol. 91, pp. 954–985, July 2007.

[8] R. Ulbricht, S. Lee, X. Jiang, K. Inoue, M. Zhang, S. Fang, R. Baughman, and A. Zakhidov, "Transparent carbon nanotube sheets as 3-D charge collectors in organic solar cells," *Solar Energy Materials and Solar Cells*, vol. 91, pp. 416–419, Mar. 2007.

[9] S. Morita, A. A. Zakhidov, and K. Yoshino, "Doping-effect of buckminster fullerene in conducting polymer: Change of absorption spectrum and quenching of luminescence," *Solid State Communications*, vol. 82, pp. 249–252, 1992.

[10] K.Yoshino, X.H.Yin, S.Morita, T.Kawai, and A.A.Zakhidov, "Effects of c60 dopping on optical properties of poly (3-alkylthiophene) by photoinduced charge transfer," *Chemical Express*, vol. 7, no. 817, 1992.

[11] S.Morita, A.A.Zakhidov, T.Kawai, H.Arake, and K.Yoshino, "Electrical conductivity and esr spectrum of buckminster fullerene doped poly (3-alkylthiophene)," *Japanese Journal of Applied Physics*, vol. 31, no. 7A, pp. L890–893, 1992.

[12] K.Yoshino, S.Morita, and A.A.Zakhidov, "Difference of doping effect of c60 and c70 in poly (3-hexylthiophene)," *Japanese Journal of Applied Physics*, no. 32L140, 1993.

[13] S.Morita, S.Kiyomatsu, X.U.Yin, A.A.Zakhidov, T.Noguchi, T.Ohnishi, and K.Yoshino, "Doping effect of buckminsterfullerene in poly(2,5-dialkoxy-p-phenylene- vinylene)," *Journal of Applied Physics*, vol. 74, p. 2860, 1993.

[14] K.Yoshino, X.H.Yin, K.Muro, S.Kiyomatsu, S.Morita, A.A.Zakhidov, T. Noguchi, and T.Ohnishi, "Marked enhancement of photoconductivity and quenching of luminescence in poly (2.5-dialkoxy-p-phenylene-vinylene) upon c60 doping," *Japanese Journal of Applied Physics*, vol. 32, no. L357, 1993.

[15] K.Yoshino, X.H.Yin, K.Muro, S. Kiyomatsu, S.Morita, A.A.Zakhidov, T.Noushi, and T.Ohnishi, "Fullerene-doped conducting polymers: Effects of enhanced photoconductivity and quenched luminescence," *Proceedings of IWEP 93*, 1993.

[16] K.Yoshino, X.H.Yin, S.Morita, T.Kawai, and A.A.Zakhidov, "Enhanced photoconductivity of c60 doped poly (3-alkylthiophene)," *Solid State Communications*, pp. 85–88, 1993.

[17] S.Morita, A.A.Zakhidov, and K.Yoshino, "Wavelength dependence of junction characteristics of poly(3-alkylthiophene) / c60 layer," *Japanese Journal of Applied Physics*, vol. 32, pp. L873–L874, 1993.

[18] K.Yoshino, S.Morita, and A.A.Zakhidov, "Difference of doping effect of c60 and c70 in poly (3-hexylthiophene)," *Japanese Journal of Applied Physics*, vol. 32L140, 1993.

[19] S.Morita, A.A.Zakhidov, and K.Yoshino, "Doping-effect of buckminster fullerene in conducting polymer: Change of absorption spectrum and quenching of luminescence," *Solid State Communications*, vol. 82, pp. 249–252, 1992.

[20] S.Morita, S. Lee, A.A.Zakhidov, and K.Yoshino, "Spectral characteristics of c60- conducting polymer junctions: Various molecular d-a type photocells," *Molecular Crystals and Liquid Crystals*, vol. 256, pp. 839–846, 1994.

[21] K.Yoshino, S.Morita, T.Akashi, K.Yoshimoto, M.Yoshida, A.Fujii, A.A.Zakhidov, K.Kikuchi, and Y.Achiba, "Doping effects of higher fullerene in conducting polymer," *Synthetic Metals*, vol. 70, pp. 1481–1482, 1995.

[22] T.Shirakawa, T.Umeda, Y.Nishihara, A.Fujii, H.Isobe, E.Nakamura, and K.Yoshino, "Doping effects of novel fullerene derivatives in conducting polymer," *Synthetic Metals*, vol. 137, pp. 1415–1416, 2003.

[23] S.Morita, S.Kiyomatsu, M.Fukuda, A.A.Zakhidov, K.Yoshino, K.Kikuchi, and Y.Achiba, "Effective photoresponse in c60-doped conducting polymer due to forbidden transition in c60," *Japanese Journal of Applied Physics*, vol. 32, pp. L1173–L1175, 1993.

[24] A.A.Zakhidov, I.M.Merhasin, and K.Yoshino, "Interaction of self-localized excitations with c60 weak dopants in conducting polymers," *Molecular Crystals and Liquid Crystals*, vol. 256, pp. 359–379, 1994.

[25] K. Yoshino, T. Akashi, S. Morita, M. Yoshida, M. Hamaguchi, K. Tada, A. Fujii, T. Kawai, S. Uto, M. Ozaki, M. Onoda, and A. A. Zakhidov, "Photophysical properties of fullerene-conducting polymer system," *Synthetic Metals*, vol. 70, pp. 1317–1320, 1995.

[26] A.A.Zakhidov, H.Araki, K.Tada, and K.Yoshino, "Fullerene-conducting polymer composites: intrinsic charge transfer processes and doping effects," *Synthetic Metals*, vol. 77, pp. 127–137, 1996.

[27] K. Yoshino, K. Tada, A. Fujii, K. Hosoda, S. Kawabe, H. Kajii, M. Hirohata, R. Hidayat, H. Araki, A. A. Zakhidov, R. Sugimoto, M. Iyoda, M. Ishikawa, and T. Masuda, "Charge transfer in fullerene-conducting polymer composite: Electronic and excitonic properties," *Fullerene Science and Technology*, vol. 5, pp. 1359–1386, 1997.

[28] A.A.Zakhidov, T.Akashi, and K.Yoshino, "Excitonic and polaron/ bipolaronic interactions in fullerene- conducting polymer systems," *Synthetic Metals*, vol. 70, pp. 1519–1522, 1995.

[29] C. Uhrich, R. Schueppel, A. Petrich, M. Pfeiffer, K. Leo, E. Brier, P. Kilickiran, and P. Baeuerle, "Organic thin-film photovoltaic cells based on oligothiophenes with reduced bandgap," *Advanced Functional Materials*, vol. 17, no. 15, pp. 2991–2999, 2007.

[30] N.Yamasaki, H.Araki, A.Zakhidov, and K.Yoshino, "Annealing effect on the superconduicting phase of sodium-nitrogen - c60 fulleride, prepared from na-azide," *Solid State Communications*, vol. 92, pp. 547–552, 1994.

[31] H.Araki, N.Yamasaki, A.A.Zakhidov, and K.Yoshino, "Evolution of superconductivity in ca-doped c60 prepared frome azide: low field microwave absorption and esr.," *Physica C*, vol. 233, pp. 242–246, 1994.

[32] *Fullerene Polymers and Fullerene Polymer Composites*, vol. 38 of *Series in Materials Science*, ch. Superconductivity of Fullerene-Conducting Polymer Composite Doped by Alkali Metals, pp. 333–368. Springer Verlag, 1999.

[33] K.Tanaka, A.A.Zakhidov, K.Yoshizawa, K.Okahara, T.Yamabe, K.Yakushi, K.Kikuchi, S.Suzuki, I.Ikemoto, and Y.Achiba, "Magnetic properties of tdae-c60 and tdae-c70: Comparative study," *Physics Letters A*, vol. 164, pp. 221–226, 1992.

[34] K. Yoshino, K. Tada, A. Fujii, E. M. Conwell, , and A. A. Zakhidov, "Novel photovoltaic devices based on donor-acceptor molecular and conducting polymer systems," *IEEE Transactions on electron devices*, vol. 44, pp. 1315–1324, 1997.

[35] A.A.Zakhidov and K.Yoshino, "Strategies for improving molecular donor-acceptor photocells: Selective doping and excitonic layers," *Synthetic Metals*, vol. 85, pp. 1299–1302, 1997.

[36] K.Yoshino, S. Lee, A.Fujii, H. Nakayama, W. Schneider, A. Naka, and M. Ishikawa, "Near ir and uv enhaced photoresponse of c60-doped semiconducting polymer photodiode," *Advanced Materials*, vol. 11, pp. 1382–1385, 1999.

[37] T.Shirakawa, T.Umeda, Y.Hashimoto, A.Fujii, and K.Yoshino, "Effect of zno layer on characteristics of conducting polymer/c60 photovoltaic cell," *Journal of Physics D: Applied Physics*, vol. 37, pp. 847–850, 2004.

[38] A. Kumar, S. Sista, and Y. Yang, "Dipole induced anomalous S-shape I-V curves in polymer solar cells," *Journal of Applied Physics*, vol. 105, no. 9, p. 094512, 2009.

[39] B. O'Regan and M. Grätzel, "A low-cost, high-efficiency solar cell based on dye-sensitized colloidal TiO2 films," *Nature*, vol. 353, pp. 737–740, Oct. 1991.

[40] C. J. Barb, F. Arendse, P. Comte, M. Jirousek, F. Lenzmann, V. Shklover, and M. Grtzel, "Nanocrystalline titanium oxide electrodes for photovoltaic applications," *Journal of the American Ceramic Society*, vol. 80, no. 12, pp. 3157–3171, 1997.

[41] W. Beek, M. Wienk, and R. Janssen, "Efficient hybrid solar cells from zinc oxide nanoparticles and a conjugated polymer," *Advanced Materials*, vol. 16, no. 12, pp. 1009–1013, 2004.

[42] W. J. E. Beek, M. M. Wienk, M. Kemerink, X. Yang, and R. A. J. Janssen, "Hybrid zinc oxide conjugated polymer bulk heterojunction solar cells.," *The journal of physical chemistry. B*, vol. 109, pp. 9505–16, May 2005.

[43] A. Kaskela, A. G. Nasibulin, M. Y. Timmermans, B. Aitchison, A. Papadimitratos, Y. Tian, Z. Zhu, H. Jiang, D. P. Brown, A. Zakhidov, and E. I. Kauppinen, "Aerosol-synthesized swcnt networks with tunable conductivity and transparency by a dry transfer technique," *Nano Letters*, vol. 10, no. 11, pp. 4349–4355, 2010.

[44] T. Takenobu, T. Takano, M. Shiraishi, Y. Murakami, M. Ata, H. Kataura, Y. Achiba, and Y. Iwasa, "Stable and controlled amphoteric doping by encapsulation of organic molecules inside carbon nanotubes.," *Nature materials*, vol. 2, pp. 683–8, Oct. 2003.

[45] J. Drechsel, "MIP-type organic solar cells incorporating phthalocyanine/fullerene mixed layers and doped wide-gap transport layers," *Organic Electronics*, vol. 5, pp. 175–186, June 2004.

[46] B. Maennig, D. Gebeyehu, P. Simon, F. Kozlowski, A. Werner, F. Li, S. Grundmann, S. Sonntag, M. Koch, K. Leo, M. Pfeiffer, H. Hoppe, D. Meissner, N. Sariciftci, I. Riedel, V. Dyakonov, J. Parisi, and J. Drechsel, "Organic p -i- n solar cells," *Applied Physics A: Materials Science & Processing*, vol. 79, pp. 1–14, June 2004.

(February 12, 2012 Accepted)